Token-level and sequence-level loss smoothing for RNN language models

Maha Elbayad[1,2] **Laurent Besacier**[1] **Jakob Verbeek**[2]

Univ. Grenoble Alpes, CNRS, Grenoble INP, Inria, LIG, LJK, F-38000 Grenoble France

[1] firstname.lastname@univ-grenoble-alpes.fr

[2] firstname.lastname@inria.fr

Abstract

Despite the effectiveness of recurrent neural network language models, their maximum likelihood estimation suffers from two limitations. It treats all sentences that do not match the ground truth as equally poor, ignoring the structure of the output space. Second, it suffers from "exposure bias": during training tokens are predicted given ground-truth sequences, while at test time prediction is conditioned on generated output sequences. To overcome these limitations we build upon the recent reward augmented maximum likelihood approach *i.e.* sequence-level smoothing that encourages the model to predict sentences close to the ground truth according to a given performance metric. We extend this approach to token-level loss smoothing, and propose improvements to the sequence-level smoothing approach. Our experiments on two different tasks, image captioning and machine translation, show that token-level and sequence-level loss smoothing are complementary, and significantly improve results.

1 Introduction

Recurrent neural networks (RNNs) have recently proven to be very effective sequence modeling tools, and are now state of the art for tasks such as machine translation (Cho et al., 2014; Sutskever et al., 2014; Bahdanau et al., 2015), image captioning (Kiros et al., 2014; Vinyals et al., 2015; Anderson et al., 2017) and automatic speech recognition (Chorowski et al., 2015; Chiu et al., 2017).

The basic principle of RNNs is to iteratively compute a vectorial sequence representation, by applying at each time-step the same trainable function to compute the new network state from the previous state and the last symbol in the sequence. These models are typically trained by maximizing the likelihood of the target sentence given an encoded source (text, image, speech).

Maximum likelihood estimation (MLE), however, has two main limitations. First, the training signal only differentiates the ground-truth target output from all other outputs. It treats all other output sequences as equally incorrect, regardless of their semantic proximity from the ground-truth target. While such a "zero-one" loss is probably acceptable for coarse grained classification of images, *e.g.* across a limited number of basic object categories (Everingham et al., 2010) it becomes problematic as the output space becomes larger and some of its elements become semantically similar to each other. This is in particular the case for tasks that involve natural language generation (captioning, translation, speech recognition) where the number of possible outputs is practically unbounded. For natural language generation tasks, evaluation measures typically do take into account structural similarity, *e.g.* based on n-grams, but such structural information is not reflected in the MLE criterion. The second limitation of MLE is that training is based on predicting the next token given the input and preceding *ground-truth* output tokens, while at test time the model predicts conditioned on the input and the so-far *generated* output sequence. Given the exponentially large output space of natural language sentences, it is not obvious that the learned RNNs generalize well beyond the relatively sparse distribution of ground-truth sequences used during MLE optimization. This phenomenon is known as "exposure bias" (Ranzato et al., 2016; Bengio et al., 2015).

MLE minimizes the KL divergence between a target Dirac distribution on the ground-truth sentence(s) and the model's distribution. In this paper, we build upon the "loss smoothing" approach by Norouzi et al. (2016), which smooths the Dirac target distribution over similar sentences, increasing the support of the training data in the output space. We make the following main contributions:

- We propose a token-level loss smoothing approach, using word-embeddings, to achieve smoothing among semantically similar terms, and we introduce a special procedure to promote rare tokens.
- For sequence-level smoothing, we propose to use restricted token replacement vocabularies, and a "lazy evaluation" method that significantly speeds up training.
- We experimentally validate our approach on the MSCOCO image captioning task and the WMT'14 English to French machine translation task, showing that on both tasks combining token-level and sequence-level loss smoothing improves results significantly over maximum likelihood baselines.

In the remainder of the paper, we review the existing methods to improve RNN training in Section 2. Then, we present our token-level and sequence-level approaches in Section 3. Experimental evaluation results based on image captioning and machine translation tasks are laid out in Section 4.

2 Related work

Previous work aiming to improve the generalization performance of RNNs can be roughly divided into three categories: those based on regularization, data augmentation, and alternatives to maximum likelihood estimation.

Regularization techniques are used to increase the smoothness of the function learned by the network, *e.g.* by imposing an ℓ_2 penalty on the network weights, also known as "weight decay". More recent approaches mask network activations during training, as in dropout (Srivastava et al., 2014) and its variants adapted to recurrent models (Pham et al., 2014; Krueger et al., 2017). Instead of masking, batch-normalization (Ioffe and Szegedy, 2015) rescales the network activations to avoid saturating the network's non-linearities. Instead of regularizing the network parameters or activations, it is also possible to directly regularize based on the entropy of the output distribution (Pereyra et al., 2017).

Data augmentation techniques improve the robustness of the learned models by applying transformations that might be encountered at test time to the training data. In computer vision, this is common practice, and implemented by, *e.g.*, scaling, cropping, and rotating training images (LeCun et al., 1998; Krizhevsky et al., 2012; Paulin et al., 2014). In natural language processing, examples of data augmentation include input noising by randomly dropping some input tokens (Iyyer et al., 2015; Bowman et al., 2015; Kumar et al., 2016), and randomly replacing words with substitutes sampled from the model (Bengio et al., 2015). Xie et al. (2017) introduced data augmentation schemes for RNN language models that leverage n-gram statistics in order to mimic Kneser-Ney smoothing of n-grams models. In the context of machine translation, Fadaee et al. (2017) modify sentences by replacing words with rare ones when this is plausible according to a pre-trained language model, and substitutes its equivalent in the target sentence using automatic word alignments. This approach, however, relies on the availability of additional monolingual data for language model training.

The *de facto* standard way to train RNN language models is maximum likelihood estimation (MLE) (Cho et al., 2014; Sutskever et al., 2014; Bahdanau et al., 2015). The sequential factorization of the sequence likelihood generates an additive structure in the loss, with one term corresponding to the prediction of each output token given the input and the preceding ground-truth output tokens. In order to directly optimize for sequence-level structured loss functions, such as measures based on n-grams like BLEU or CIDER, Ranzato et al. (2016) use reinforcement learning techniques that optimize the expectation of a sequence-level reward. In order to avoid early convergence to poor local optima, they pre-train the model using MLE.

Leblond et al. (2018) build on the learning to search approach to structured prediction (Daumé III et al., 2009; Chang et al., 2015) and adapts it to RNN training. The model generates candidate sequences at each time-step using all possible tokens, and scores these at sequence-level to derive a training signal for each time step. This leads to an approach that is structurally close to MLE, but computationally expensive. Norouzi et al. (2016) introduce a reward augmented maximum likelihood (RAML) approach, that incorporates a notion of sequence-level reward without facing the difficulties of reinforcement learning. They define a target distribution over output sentences using a soft-max over the reward over all possible outputs. Then, they minimize the KL divergence between the target distribution and the model's output distribution. Training with a general reward distribution is similar to MLE training, except that we use multiple sentences sampled from the target distribution instead of only the ground-truth sentences.

In our work, we build upon the work of Norouzi et al. (2016) by proposing improvements to sequence-level smoothing, and extending it to token-level smoothing. Our token-level smoothing approach is related to the label smoothing approach of Szegedy et al. (2016) for image classification. Instead of maximizing the probability of the correct class, they train the model to predict the correct class with a large probability and all other classes with a small uniform probability. This regularizes the model by preventing overconfident predictions. In natural language generation with large vocabularies, preventing such "narrow" over-confident distributions is imperative, since for many tokens there are nearly interchangeable alternatives.

3 Loss smoothing for RNN training

We briefly recall standard recurrent neural network training, before presenting sequence-level and token-level loss smoothing below.

3.1 Maximum likelihood RNN training

We are interested in modeling the conditional probability of a sequence $y = (y_1, \dots, y_T)$ given a conditioning observation x,

$$p_\theta(y|x) = \prod_{t=1}^{T} p_\theta(y_t|x, y_{<t}), \tag{1}$$

where $y_{<t} = (y_1, \dots, y_{t-1})$, the model parameters are given by θ, and x is a source sentence or an image in the contexts of machine translation and image captioning, respectively.

In a recurrent neural network, the sequence y is predicted based on a sequence of states h_t,

$$p_\theta(y_t|x, y_{<t}) = p_\theta(y_t|h_t), \tag{2}$$

where the RNN state is computed recursively as

$$h_t = \begin{cases} f_\theta(h_{t-1}, y_{t-1}, x) & \text{for } t \in \{1, ..T\}, \\ g_\theta(x) & \text{for } t = 0. \end{cases} \tag{3}$$

The input is encoded by g_θ and used to initialize the state sequence, and f_θ is a non-linear function that updates the state given the previous state h_{t-1}, the last output token y_{t-1}, and possibly the input x. The state update function can take different forms, the ones including gating mechanisms such as LSTMs (Hochreiter and Schmidhuber, 1997) and GRUs (Chung et al., 2014) are particularly effective to model long sequences.

In standard teacher-forced training, the hidden states will be computed by forwarding the ground truth sequence y^* *i.e.* in Eq. (3), the RNN has access to the true previous token y^*_{t-1}. In this case we will note the hidden states h^*_t.

Given a ground-truth target sequence y^*, maximum likelihood estimation (MLE) of the network parameters θ amounts to minimizing the loss

$$\ell_{\text{MLE}}(y^*, x) = -\ln p_\theta(y^*|x) \tag{4}$$

$$= -\sum_{t=1}^{T} \ln p_\theta(y^*_t|h^*_t). \tag{5}$$

The loss can equivalently be expressed as the KL-divergence between a Dirac centered on the target output (with $\delta_a(x) = 1$ at $x = a$ and 0 otherwise) and the model distribution, either at the sequence-level or at the token-level:

$$\ell_{\text{MLE}}(y^*, x) = D_{\text{KL}}\big(\delta_{y^*}||p_\theta(y|x)\big) \tag{6}$$

$$= \sum_{t=1}^{T} D_{\text{KL}}\big(\delta_{y^*_t}||p_\theta(y_t|h^*_t)\big). \tag{7}$$

Loss smoothing approaches considered in this paper consist in replacing the Dirac on the ground-truth sequence with distributions with larger support. These distributions can be designed in such a manner that they reflect which deviations from ground-truth predictions are preferred over others.

3.2 Sequence-level loss smoothing

The reward augmented maximum likelihood approach of Norouzi et al. (2016) consists in replacing the sequence-level Dirac δ_{y^*} in Eq. (6) with a distribution

$$r(y|y^*) \propto \exp r(y, y^*)/\tau, \tag{8}$$

where $r(y, y^*)$ is a "reward" function that measures the quality of sequence y w.r.t. y^*, *e.g.* metrics used for evaluation of natural language processing tasks can be used, such as BLEU (Papineni et al., 2002) or CIDEr (Vedantam et al., 2015). The temperature parameter τ controls the concentration of the distribution around y^*. When $m > 1$ ground-truth sequences are paired with the same input x, the reward function can be adapted to fit this setting and be defined as $r(y, \{y^{*(1)}, \ldots, y^{*(m)}\})$. The sequence-level smoothed loss function is then given by

$$\begin{aligned}\ell_{\text{Seq}}(y^*, x) &= D_{\text{KL}}\big(r(y|y^*)||p_\theta(y|x)\big) \\ &= H(r(y|y^*)) - \mathbb{E}_r[\ln p_\theta(y|x)]\,, \quad (9)\end{aligned}$$

where the entropy term $H(r(y|y^*))$ does not depend on the model parameters θ.

In general, expectation in Eq. (9) is intractable due to the exponentially large output space, and replaced with a Monte-Carlo approximation:

$$\mathbb{E}_r[-\ln p_\theta(y|x)] \approx -\sum_{l=1}^{L} \ln p_\theta(y^l|x). \quad (10)$$

Stratified sampling. Norouzi et al. (2016) show that when using the Hamming or edit distance as a reward, we can sample directly from $r(y|y^*)$ using a stratified sampling approach. In this case sampling proceeds in three stages. (i) Sample a distance d from $\{0, \ldots, T\}$ from a prior distribution on d. (ii) Uniformly select d positions in the sequence to be modified. (iii) Sample the d substitutions uniformly from the token vocabulary.

Details on the construction of the prior distribution on d for a reward based on the Hamming distance can be found in Appendix A.

Importance sampling. For a reward based on BLEU or CIDEr , we cannot directly sample from $r(y|y^*)$ since the normalizing constant, or "partition function", of the distribution is intractable to compute. In this case we can resort to importance sampling. We first sample L sequences y^l from a tractable proposal distribution $q(y|y^*)$. We then compute the importance weights

$$\omega_l \approx \frac{r(y^l|y^*)/q(y^l|y^*)}{\sum_{k=1}^{L} r(y^k|y^*)/q(y^k|y^*)}, \quad (11)$$

where $r(y^k|y^*)$ is the un-normalized reward distribution in Eq. (8). We finally approximate the expectation by reweighing the samples in the Monte Carlo approximation as

$$\mathbb{E}_r[-\ln p_\theta(y|x)] \approx -\sum_{l=1}^{L} \omega_l \ln p_\theta(y^l|x). \quad (12)$$

In our experiments we use a proposal distribution based on the Hamming distance, which allows for tractable stratified sampling, and generates sentences that do not stray away from the ground truth.

We propose two modifications to the sequence-level loss smoothing of Norouzi et al. (2016): sampling to a restricted vocabulary (described in the following paragraph) and lazy sequence-level smoothing (described in section 3.4).

Restricted vocabulary sampling. In the stratified sampling method for Hamming and edit distance rewards, instead of drawing from the large vocabulary $\mathcal{V}$, containing typically in the order of 10^4 words or more, we can restrict ourselves to a smaller subset $\mathcal{V}_{sub}$ more adapted to our task. We considered three different possibilities for $\mathcal{V}_{sub}$.

$\mathcal{V}$: the full vocabulary from which we sample uniformly (default), or draw from our token-level smoothing distribution defined below in Eq. (13).

$\mathcal{V}_{refs}$: uniformly sample from the set of tokens that appear in the ground-truth sentence(s) associated with the current input.

$\mathcal{V}_{batch}$: uniformly sample from the tokens that appear in the ground-truth sentences across all inputs that appear in a given training mini-batch.

Uniformly sampling from $\mathcal{V}_{batch}$ has the effect of boosting the frequencies of words that appear in many reference sentences, and thus approximates to some extent sampling substitutions from the uni-gram statistics of the training set.

3.3 Token-level loss smoothing

While the sequence-level smoothing can be directly based on performance measures of interest such as BLEU or CIDEr, the support of the smoothed distribution is limited to the number of samples drawn during training. We propose smoothing the token-level Diracs $\delta_{y_t^*}$ in Eq. (7) to increase its support to similar tokens. Since we apply smoothing to each of the tokens independently, this approach implicitly increases the support to an exponential number of sequences, unlike the sequence-level smoothing approach. This comes at the price, however, of a naive token-level independence assumption in the smoothing.

We define the smoothed token-level distribution, similar as the sequence-level one, as a softmax over a token-level "reward" function,

$$r(y_t|y_t^*) \propto \exp r(y_t, y_t^*)/\tau, \quad (13)$$

where τ is again a temperature parameter. As a token-level reward $r(y_t, y_t^*)$ we use the cosine similarity between y_t and y_t^* in a semantic word-embedding space. In our experiments we use GloVe (Pennington et al., 2014); preliminary experiments with word2vec (Mikolov et al., 2013) yielded somewhat worse results.

Promoting rare tokens. We can further improve the token-level smoothing by promoting rare tokens. To do so, we penalize frequent tokens when smoothing over the vocabulary, by subtracting $\beta\,\mathrm{freq}(y_t)$ from the reward, where $\mathrm{freq}(\cdot)$ denotes the term frequency and β is a non-negative weight. This modification encourages frequent tokens into considering the rare ones. We experimentally found that it is also beneficial for rare tokens to boost frequent ones, as they tend to have mostly rare tokens as neighbors in the word-embedding space. With this in mind, we define a new token-level reward as:

$$r^{\mathrm{freq}}(y_t, y_t^*) = r(y_t, y_t^*) - \beta \min\left(\frac{\mathrm{freq}(y_t)}{\mathrm{freq}(y_t^*)}, \frac{\mathrm{freq}(y_t^*)}{\mathrm{freq}(y_t)}\right), \tag{14}$$

where the penalty term is strongest if both tokens have similar frequencies.

3.4 Combining losses

In both loss smoothing methods presented above, the temperature parameter τ controls the concentration of the distribution. As τ gets smaller the distribution peaks around the ground-truth, while for large τ the uniform distribution is approached. We can, however, not separately control the spread of the distribution and the mass reserved for the ground-truth output. We therefore introduce a second parameter $\alpha \in [0, 1]$ to interpolate between the Dirac on the ground-truth and the smooth distribution. Using $\bar{\alpha} = 1 - \alpha$, the sequence-level and token-level loss functions are then defined as

$$\begin{aligned}\ell^{\alpha}_{\text{Seq}}(y^*, x) &= \alpha \ell_{\text{Seq}}(y^*, x) + \bar{\alpha}\ell_{\text{MLE}}(y^*, x) \quad (15)\\ &= \alpha \mathbb{E}_r[\ell_{\text{MLE}}(y, x)] + \bar{\alpha}\ell_{\text{MLE}}(y^*, x)\\ \ell^{\alpha}_{\text{Tok}}(y^*, x) &= \alpha \ell_{\text{Tok}}(y^*, x) + \bar{\alpha}\ell_{\text{MLE}}(y^*, x) \quad (16)\end{aligned}$$

To benefit from both sequence-level and token-level loss smoothing, we also combine them by applying token-level smoothing to the different sequences sampled for the sequence-level smoothing. We introduce two mixing parameters α_1 and α_2. The first controls to what extent sequence-level smoothing is used, while the second controls to what extent token-level smoothing is used. The combined loss is defined as

$$\begin{aligned}\ell^{\alpha_1,\alpha_2}_{\text{Seq, Tok}}(y^*, x, r) &= \alpha_1 \mathbb{E}_r[\ell_{\text{Tok}}(y, x)] + \bar{\alpha}_1 \ell_{\text{Tok}}(y^*, x)\\ &= \alpha_1 \mathbb{E}_r[\alpha_2 \ell_{\text{Tok}}(y, x) + \bar{\alpha}_2 \ell_{\text{MLE}}(y, x)]\\ &\quad + \bar{\alpha}_1(\alpha_2 \ell_{\text{Tok}}(y^*, x) + \bar{\alpha}_2 \ell_{\text{MLE}}(y^*, x)).\end{aligned} \tag{17}$$

In our experiments, we use held out validation data to set mixing and temperature parameters.

Algorithm 1 Sequence-level smoothing algorithm

Input: x, y^*
Output: $\ell^{\alpha}_{\text{seq}}(x, y^*)$
  Encode x to initialize the RNN
  Forward y^* in the RNN to compute the hidden states h_t^*
  Compute the MLE loss $\ell_{\text{MLE}}(y^*, x)$
  for $l \in \{1, \dots, L\}$ **do**
    Sample $y^l \sim r(|y^*)$
    if Lazy **then**
      Compute $\ell(y^l, x) = -\sum_t \log p_\theta(y_t^l | h_t^*)$
    else
      Forward y^l in the RNN to get its hidden states h_t^l
      Compute $\ell(y^l, x) = \ell_{\text{MLE}}(y^l, x)$
    end if
  end for
  $\ell^{\alpha}_{\text{Seq}}(x, y^*) = \bar{\alpha}\ell_{\text{MLE}}(y^*, x) + \frac{\alpha}{L}\sum_l \ell(y^l, x)$

Lazy sequence smoothing. Although sequence-level smoothing is computationally efficient compared to reinforcement learning approaches (Ranzato et al., 2016; Rennie et al., 2017), it is slower compared to MLE. In particular, we need to forward each of the samples y^l through the RNN in teacher-forcing mode so as to compute its hidden states h_t^l, which are used to compute the sequence MLE loss as

$$\ell_{\text{MLE}}(y^l, x) = -\sum_{t=1}^{T} \ln p_\theta(y_t^l | h_t^l). \tag{18}$$

To speed up training, and since we already forward the ground truth sequence in the RNN to evaluate the MLE part of $\ell^{\alpha}_{\text{Seq}}(y^*, x)$, we propose to use the same hidden states h_t^* to compute both the MLE and the sequence-level smoothed loss. In this case:

$$\ell_{\text{lazy}}(y^l, x) = -\sum_{t=1}^{T} \ln p_\theta(y_t^l | h_t^*) \tag{19}$$

In this manner, we only have a single instead of $L + 1$ forwards-passes in the RNN. We provide the pseudo-code for training in Algorithm 1.

			Without attention			With attention		
Loss	Reward	$\mathcal{V}_{sub}$	BLEU-1	BLEU-4	CIDER	BLEU-1	BLEU-4	CIDER
MLE			70.63	30.14	93.59	73.40	33.11	101.63
MLE + γH			70.79	30.29	93.61	72.68	32.15	99.77
Tok	Glove sim		71.94	31.27	95.79	73.49	32.93	102.33
Tok	Glove sim r^{freq}		72.39	31.76	97.47	74.01	33.25	102.81
Seq	Hamming	$\mathcal{V}$	71.76	31.16	96.37	73.12	32.71	101.25
Seq	Hamming	$\mathcal{V}_{batch}$	71.46	31.15	**96.53**	73.26	**32.73**	101.90
Seq	Hamming	$\mathcal{V}_{refs}$	**71.80**	**31.63**	96.22	**73.53**	32.59	**102.33**
Seq, lazy	Hamming	$\mathcal{V}$	70.81	30.43	94.26	73.29	32.81	101.58
Seq, lazy	Hamming	$\mathcal{V}_{batch}$	71.85	31.13	**96.65**	73.43	32.95	**102.03**
Seq, lazy	Hamming	$\mathcal{V}_{refs}$	**71.96**	**31.23**	95.34	**73.53**	**33.09**	101.89
Seq	CIDER	$\mathcal{V}$	71.05	30.46	94.40	73.08	32.51	101.84
Seq	CIDER	$\mathcal{V}_{batch}$	71.51	31.17	95.78	**73.50**	**33.04**	**102.98**
Seq	CIDER	$\mathcal{V}_{refs}$	**71.93**	**31.41**	**96.81**	73.42	32.91	102.23
Seq, lazy	CIDER	$\mathcal{V}$	71.43	**31.18**	**96.32**	73.55	**33.19**	**102.94**
Seq, lazy	CIDER	$\mathcal{V}_{batch}$	71.47	31.00	95.56	73.18	32.60	101.30
Seq, lazy	CIDER	$\mathcal{V}_{refs}$	**71.82**	31.06	95.66	**73.92**	33.10	102.64
Tok-Seq	Hamming	$\mathcal{V}$	70.79	30.43	96.34	73.68	32.87	101.11
Tok-Seq	Hamming	$\mathcal{V}_{batch}$	72.28	31.65	96.73	73.86	33.32	102.90
Tok-Seq	Hamming	$\mathcal{V}_{refs}$	72.69	32.30	98.01	73.56	33.00	101.72
Tok-Seq	CIDER	$\mathcal{V}$	70.80	30.55	96.89	73.31	32.40	100.33
Tok-Seq	CIDER	$\mathcal{V}_{batch}$	72.13	31.71	96.92	73.61	32.67	101.41
Tok-Seq	CIDER	$\mathcal{V}_{refs}$	**73.08**	**32.82**	**99.92**	**74.28**	**33.34**	**103.81**

Table 1: MS-COCO 's test set evaluation measures.

4 Experimental evaluation

In this section, we compare sequence prediction models trained with maximum likelihood (MLE) with our token and sequence-level loss smoothing on two different tasks: image captioning and machine translation.

4.1 Image captioning

4.1.1 Experimental setup.

We use the MS-COCO datatset (Lin et al., 2014), which consists of 82k training images each annotated with five captions. We use the standard splits of Karpathy and Li (2015), with 5k images for validation, and 5k for test. The test set results are generated via beam search (beam size 3) and are evaluated with the MS-COCO captioning evaluation tool. We report CIDER and BLEU scores on this internal test set. We also report results obtained on the official MS-COCO server that additionally measures METEOR (Denkowski and Lavie, 2014) and ROUGE-L (Lin, 2004). We experiment with both non-attentive LSTMs (Vinyals et al., 2015) and the ResNet baseline of the state-of-the-art top-down attention (Anderson et al., 2017).

The MS-COCO vocabulary consists of 9,800 words that occur at least 5 times in the training set. Additional details and hyperparameters can be found in Appendix B.1.

4.1.2 Results and discussion

Restricted vocabulary sampling In this section, we evaluate the impact of the vocabulary subset from which we sample the modified sentences for sequence-level smoothing. We experiment with two rewards: CIDER , which scores w.r.t. all five available reference sentences, and Hamming distance reward taking only a single reference into account. For each reward we train our (Seq) models with each of the three subsets detailed previously in Section 3.2, Restricted vocabulary sampling.

From the results in Table 1 we note that for the inattentive models, sampling from $\mathcal{V}_{refs}$ or $\mathcal{V}_{batch}$ has a better performance than sampling from the full vocabulary on all metrics. In fact, using these subsets introduces a useful bias to the model and improves performance. This improvement is most notable using the CIDER reward that scores candidate sequences w.r.t. to multiple references, which stabilizes the scoring of the candidates.

With an attentive decoder, no matter the reward, re-sampling sentences with words from $\mathcal{V}_{ref}$ rather than the full vocabulary $\mathcal{V}$ is better for both reward functions, and all metrics. Additional experimental results, presented in Appendix B.2, obtained with a BLEU-4 reward, in its single and

	BLEU-1		BLEU-2		BLEU-3		BLEU-4		METEOR		ROUGE-L		CIDEr		SPICE	
	c5	c40	c5	c40	c5	c40	c5	c40	c5	c40	c5	c40	c5	c40	c5	c40
Google NIC^{+} (Vinyals et al., 2015)	71.3	89.5	54.2	80.2	40.7	69.4	30.9	58.7	25.4	34.6	53.0	68.2	94.3	94.6	18.2	63.6
Hard-Attention (Xu et al., 2015)	70.5	88.1	52.8	77.9	38.3	65.8	27.7	53.7	24.1	32.2	51.6	65.4	86.5	89.3	17.2	59.8
ATT-FCN^{+} (You et al., 2016)	73.1	90.0	56.5	81.5	42.4	70.9	31.6	59.9	25.0	33.5	53.5	68.2	94.3	95.8	18.2	63.1
Review Net^{+} (Yang et al., 2016)	72.0	90.0	55.0	81.2	41.4	70.5	31.3	59.7	25.6	34.7	53.3	68.6	96.5	96.9	18.5	64.9
Adaptive^{+} (Lu et al., 2017)	74.8	92.0	58.4	84.5	44.4	74.4	33.6	63.7	26.4	35.9	55.0	70.5	104.2	105.9	19.7	67.3
SCST:Att2all$^{+\dagger}$ (Rennie et al., 2017)	78.1	93.7	61.9	86.0	47.0	75.9	35.2	64.5	27.0	35.5	56.3	70.7	114.7	116.7	-	-
LSTM-A3$^{+\dagger\circ}$ (Yao et al., 2017)	78.7	93.7	62.7	86.7	47.6	76.5	35.6	65.2	27.0	35.4	56.4	70.5	116	118	-	-
Up-Down$^{+\dagger\circ}$ (Anderson et al., 2017)	80.2	95.2	64.1	88.8	49.1	79.4	36.9	68.5	27.6	36.7	57.1	72.4	117.9	120.5	-	-
Ours: Tok-Seq CIDEr	72.6	89.7	55.7	80.9	41.2	69.8	30.2	58.3	25.5	34.0	53.5	68.0	96.4	99.4	-	-
Ours: Tok-Seq CIDEr $^{+}$	74.9	92.4	58.5	84.9	44.8	75.1	34.3	64.7	26.5	36.1	55.2	71.1	103.9	104.2	-	-

Table 2: MS-COCO 's server evaluation . ($^{+}$) for ensemble submissions, (†) for submissions with CIDEr optimization and ($^{\circ}$) for models using additional data.

multiple references variants, further corroborate this conclusion.

Lazy training. From the results of Table 1, we see that lazy sequence-level smoothing is competitive with exact non-lazy sequence-level smoothing, while requiring roughly equivalent training time as MLE. We provide detailed timing results in Appendix B.3.

Overall For reference, we include in Table 1 baseline results obtained using MLE, and our implementation of MLE with entropy regularization (MLE+γH) (Pereyra et al., 2017), as well as the RAML approach of Norouzi et al. (2016) which corresponds to sequence-level smoothing based on the Hamming reward and sampling replacements from the full vocabulary (Seq, Hamming, $\mathcal{V}$)

We observe that entropy smoothing is not able to improve performance much over MLE for the model without attention, and even deteriorates for the attention model. We improve upon RAML by choosing an adequate subset of vocabulary for substitutions.

We also report the performances of token-level smoothing, where the promotion of rare tokens boosted the scores in both attentive and non-attentive models.

For sequence-level smoothing, choosing a task-relevant reward with importance sampling yielded better results than plain Hamming distance.

Moreover, we used the two smoothing schemes (Tok-Seq) and achieved the best results with CIDEr as a reward for sequence-level smoothing combined with a token-level smoothing that promotes rare tokens improving CIDEr from 93.59 (MLE) to 99.92 for the model without attention, and improving from 101.63 to 103.81 with attention.

Qualitative results. In Figure 1 we showcase captions obtained with MLE and our three variants of smoothing *i.e.* token-level (Tok), sequence-level (Seq) and the combination (Tok-Seq). We note that the sequence-level smoothing tend to generate lengthy captions overall, which is maintained in the combination. On the other hand, the token-level smoothing allows for a better recognition of objects in the image that stems from the robust training of the classifier *e.g.* the 'cement block' in the top right image or the carrots in the bottom right. More examples are available in Appendix B.4

Comparison to the state of the art. We compare our model to state-of-the-art systems on the MS-COCO evaluation server in Table 2. We submitted a single model (Tok-Seq, CIDEr , $\mathcal{V}_{refs}$) as well as an ensemble of five models with different initializations trained on the training set plus 35k images from the dev set (a total of 117k images) to the MS-COCO server. The three best results on the server (Rennie et al., 2017; Yao et al., 2017; Anderson et al., 2017) are trained in two stages where they first train using MLE, before switching to policy gradient methods based on CIDEr. Anderson et al. (2017) reported an increase of 5.8% of CIDEr on the test split after the CIDEr optimization. Moreover, Yao et al. (2017) uses additional information about image regions to train the attributes classifiers, while Anderson et al. (2017) pre-trains its bottom-up attention model on the Visual Genome dataset (Krishna et al., 2017). Lu et al. (2017); Yao et al. (2017) use the same CNN encoder as ours (ResNet-152), (Vinyals et al., 2015; Yang et al., 2016) use Inception-v3 (Szegedy et al., 2016) for image encoding and Rennie et al. (2017); Anderson et al.

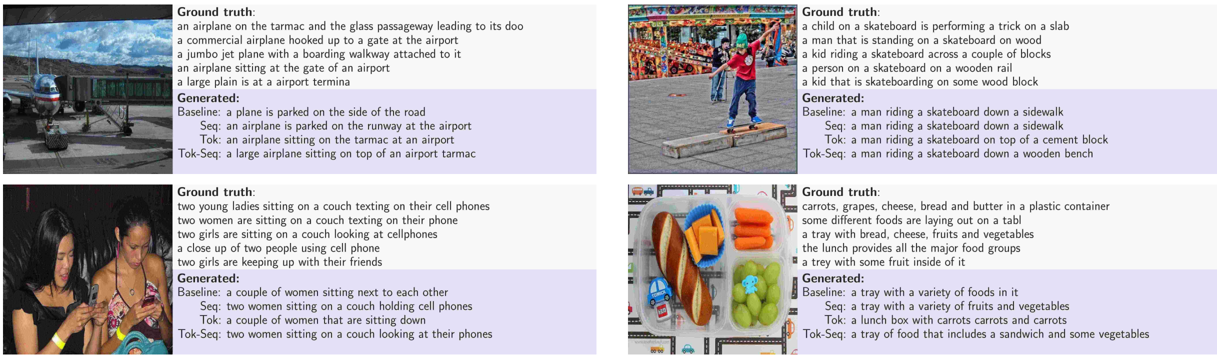

Figure 1: Examples of generated captions with the baseline MLE and our models with attention.

(2017) use Resnet-101, both of which have similar performances to ResNet-152 on ImageNet classification (Canziani et al., 2016).

4.2 Machine translation

4.2.1 Experimental setup.

For this task we validate the effectiveness of our approaches on two different datasets. The first is WMT'14 English to French, in its filtered version, with 12M sentence pairs obtained after dynamically selecting a "clean" subset of 348M words out of the original "noisy" 850M words (Bahdanau et al., 2015; Cho et al., 2014; Sutskever et al., 2014). The second benchmark is IWSLT'14 German to English consisting of around 150k pairs for training. In all our experiments we use the attentive model of (Bahdanau et al., 2015) The hyperparameters of each of these models as well as any additional pre-processing can be found in Appendix C.1

To assess the translation quality we report the BLEU-4 metric.

4.2.2 Results and analysis

Loss	Reward	$\mathcal{V}_{sub}$	WMT'14	IWSLT'14
MLE			30.03	27.55
tok	Glove sim		30.16	27.69
tok	Glove sim r^{freq}		30.19	27.83
Seq	Hamming	$\mathcal{V}$	30.85	27.98
Seq	Hamming	$\mathcal{V}_{batch}$	31.18	28.54
Seq	BLEU-4	$\mathcal{V}_{batch}$	31.29	28.56
Tok-Seq	Hamming	$\mathcal{V}_{batch}$	31.36	28.70
Tok-Seq	BLEU-4	$\mathcal{V}_{batch}$	31.39	28.74

Table 3: Tokenized BLEU score on WMT'14 En-Fr evaluated on the news-test-2014 set. And Tokenzied, case-insensitive BLEU on IWSLT'14 De-En.

We present our results in Table 3. On both benchmarks, we improve on both MLE and RAML approach of Norouzi et al. (2016) (Seq, Hamming, $\mathcal{V}$): using the smaller batch-vocabulary for replacement improves results, and using importance sampling based on BLEU-4 further boosts results. In this case, unlike in the captioning experiment, token-level smoothing brings smaller improvements. The combination of both smoothing approaches gives best results, similar to what was observed for image captioning, improving the MLE BLEU-4 from 30.03 to 31.39 on WMT'14 and from 27.55 to 28.74 on IWSLT'14. The outputs of our best model are compared to the MLE in some examples showcased in Appendix C.

5 Conclusion

We investigated the use of loss smoothing approaches to improve over maximum likelihood estimation of RNN language models. We generalized the sequence-level smoothing RAML approach of Norouzi et al. (2016) to the token-level by smoothing the ground-truth target across semantically similar tokens. For the sequence-level, which is computationally expensive, we introduced an efficient "lazy" evaluation scheme, and introduced an improved re-sampling strategy. Experimental evaluation on image captioning and machine translation demonstrates the complementarity of sequence-level and token-level loss smoothing, improving over both the maximum likelihood and RAML.

Acknowledgment. This work has been partially supported by the grant ANR-16-CE23-0006 "Deep in France" and LabEx PERSYVAL-Lab (ANR-11-LABX-0025-01).

References

P. Anderson, X. He, C. Buehler, D. Teney, M. Johnson, S. Gould, and L. Zhang. 2017. Bottom-up and top-down attention for image captioning and visual question answering. *arXiv preprint arXiv:1707.07998*.

D. Bahdanau, K. Cho, and Y. Bengio. 2015. Neural machine translation by jointly learning to align and translate. In *ICLR*.

S. Bengio, O. Vinyals, N. Jaitly, and N. Shazeer. 2015. Scheduled sampling for sequence prediction with recurrent neural networks. In *NIPS*.

S. Bowman, L. Vilnis, O. Vinyals, A. Dai, R. Jozefowicz, and S. Bengio. 2015. Generating sentences from a continuous space. In *CoNLL*.

A. Canziani, A. Paszke, and E. Culurciello. 2016. An analysis of deep neural network models for practical applications. *arXiv preprint arXiv:1605.07678*.

K.-W. Chang, A. Krishnamurthy, A. Agarwal, H. Daumé III, and J. Langford. 2015. Learning to search better than your teacher. In *ICML*.

C.-C. Chiu, T. Sainath, Y. Wu, R. Prabhavalkar, P. Nguyen, Z. Chen, A. Kannan, R.-J. Weiss, K. Rao, E. Gonina, N. Jaitly, B. Li, J. Chorowski, and M. Bacchiani. 2017. State-of-the-art speech recognition with sequence-to-sequence models. *arXiv preprint arXiv:1712.01769*.

K. Cho, B. van Merrienboer, Ç. Gülçehre, D. Bahdanau, F. Bougares, H. Schwenk, and Y. Bengio. 2014. Learning phrase representations using RNN encoder-decoder for statistical machine translation. In *Empirical Methods in Natural Language Processing*.

J. Chorowski, D. Bahdanau, D. Serdyuk, K. Cho, and Y. Bengio. 2015. Attention-based models for speech recognition. In *NIPS*.

J. Chung, C. Gulcehre, K. Cho, and Y. Bengio. 2014. Empirical evaluation of gated recurrent neural networks on sequence modeling. In *NIPS Deep Learning Workshop*.

H. Daumé III, J. Langford, and D. Marcu. 2009. Search-based structured prediction. *Machine Learning*, 75(3):297–325.

M. Denkowski and A. Lavie. 2014. Meteor universal: Language specific translation evaluation for any target language. In *Workshop on statistical machine translation*.

M. Everingham, L. van Gool, C. Williams, J. Winn, and A. Zisserman. 2010. The pascal visual object classes (VOC) challenge. *IJCV*, 88(2):303–338.

M. Fadaee, A. Bisazza, and C. Monz. 2017. Data augmentation for low-resource neural machine translation. In *ACL*.

K. He, X. Zhang, S. Ren, and J. Sun. 2016. Deep residual learning for image recognition. In *CVPR*.

S. Hochreiter and J. Schmidhuber. 1997. Long short-term memory. *Neural Computation*, 9(8):1735–1780.

S. Ioffe and C. Szegedy. 2015. Batch normalization: Accelerating deep network training by reducing internal covariate shift. In *ICML*.

M. Iyyer, V. Manjunatha, J. Boyd-Graber, and H. Daumé III. 2015. Deep unordered composition rivals syntactic methods for text classification. In *ACL*.

A. Karpathy and Fei-Fei Li. 2015. Deep visual-semantic alignments for generating image descriptions. In *CVPR*.

D. Kingma and J. Ba. 2015. Adam: A method for stochastic optimization. In *ICLR*.

R. Kiros, R. Salakhutdinov, and R. Zemel. 2014. Multimodal neural language models. In *ICML*.

R. Krishna, Y. Zhu, O. Groth, J. Johnson, K. Hata, J. Kravitz, S. Chen, Y. Kalantidis, L.-J. Li, D. Shamma, M. Bernstein, and L. Fei-Fei. 2017. Visual genome: Connecting language and vision using crowdsourced dense image annotations. *IJCV*, 123(1):32–73.

A. Krizhevsky, I. Sutskever, and G. Hinton. 2012. Imagenet classification with deep convolutional neural networks. In *NIPS*.

D. Krueger, T. Maharaj, J. Kramár, M. Pezeshki, N. Ballas, N. Ke, A. Goyal, Y. Bengio, H. Larochelle, A. Courville, and C. Pal. 2017. Zoneout: Regularizing RNNs by randomly preserving hidden activations. In *ICLR*.

A. Kumar, O. Irsoy, P. Ondruska, M. Iyyer, J. Bradbury, I. Gulrajani, V. Zhong, R. Paulus, and R. Socher. 2016. Ask me anything: Dynamic memory networks for natural language processing. In *ICML*.

R. Leblond, J.-B. Alayrac, A. Osokin, and S. Lacoste-Julien. 2018. SeaRnn: Training RNNs with global-local losses. In *ICLR*.

Y. LeCun, L. Bottou, Y. Bengio, and P. Haffner. 1998. Gradient-based learning applied to document recognition. *Proceedings of the IEEE*, pages 2278–2324.

C.-Y. Lin. 2004. Rouge: a package for automatic evaluation of summaries. In *ACL Workshop Text Summarization Branches Out*.

T.-Y. Lin, M. Maire, S. Belongie, L. Bourdev, R. Girshick, J. Hays, P. Perona, D. Ramanan, P. Dollár, and C. Zitnick. 2014. Microsoft COCO: common objects in context. In *ECCV*.

J. Lu, C. Xiong, D. Parikh, and R. Socher. 2017. Knowing when to look: Adaptive attention via a visual sentinel for image captioning. In *CVPR*.

T. Mikolov, K. Chen, G. Corrado, and J. Dean. 2013. Efficient estimation of word representations in vector space. In *ICLR*.

M. Norouzi, S. Bengio, Z. Chen, N. Jaitly, M. Schuster, Y. Wu, and D. Schuurmans. 2016. Reward augmented maximum likelihood for neural structured prediction. In *NIPS*.

K. Papineni, S. Roukos, T. Ward, and W.-J. Zhu. 2002. BLEU: a method for automatic evaluation of machine translation. In *Proceedings of the Annual Meeting of the Association for Computational Linguistics*.

M. Paulin, J. Revaud, Z. Harchaoui, F. Perronnin, and C. Schmid. 2014. Transformation pursuit for image classification. In *CVPR*.

M. Pedersoli, T. Lucas, C. Schmid, and J. Verbeek. 2017. Areas of attention for image captioning. In *ICCV*.

J. Pennington, R. Socher, and C. Manning. 2014. GloVe: Global vectors for word representation. In *Empirical Methods in Natural Language Processing*.

G. Pereyra, G. Tucker, J. Chorowski, L. Kaiser, and G. Hinton. 2017. Regularizing neural networks by penalizing confident output distributions. In *ICLR*.

V. Pham, T. Bluche, C. Kermorvant, and J. Louradour. 2014. Dropout improves recurrent neural networks for handwriting recognition. In *Frontiers in Handwriting Recognition*.

M. Ranzato, S. Chopra, M. Auli, and W. Zaremba. 2016. Sequence level training with recurrent neural networks. In *ICLR*.

S. Rennie, E. Marcheret, Y. Mroueh, J. Ross, and V. Goel. 2017. Self-critical sequence training for image captioning. In *CVPR*.

N. Srivastava, G. Hinton, A. Krizhevsky, I. Sutskever, and R. Salakhutdinov. 2014. Dropout: A simple way to prevent neural networks from overfitting. *JMLR*.

I. Sutskever, O. Vinyals, and Q. Le. 2014. Sequence to sequence learning with neural networks. In *NIPS*.

C. Szegedy, V. Vanhoucke, S. Ioffe, J. Shlens, and Z. Wojna. 2016. Rethinking the inception architecture for computer vision. In *CVPR*.

R. Vedantam, C. Zitnick, and D. Parikh. 2015. CIDEr: Consensus-based image description evaluation. In *CVPR*.

O. Vinyals, A. Toshev, S. Bengio, and D. Erhan. 2015. Show and tell: A neural image caption generator. In *CVPR*.

Z. Xie, S. Wang, J. Li, D. Lévy, A. Nie, D. Jurafsky, and A. Ng. 2017. Data noising as smoothing in neural network language models. In *ICLR*.

K. Xu, J. Ba, R. Kiros, K. Cho, A. Courville, R. Salakhutdinov, R. Zemel, and Y. Bengio. 2015. Show, attend and tell: Neural image caption generation with visual attention. In *ICML*.

Z. Yang, Y. Yuan, Y. Wu, R. Salakhutdinov, and W. Cohen. 2016. Encode, review, and decode: Reviewer module for caption generation. In *NIPS*.

T. Yao, Y. Pan, Y. Li, Z. Qiu, and T. Mei. 2017. Boosting image captioning with attributes. In *ICLR*.

Q. You, H. Jin, Z. Wang, C. Fang, and J. Luo. 2016. Image captioning with semantic attention. In *CVPR*.

A Stratified sampling of the Hamming distance

Norouzi et al. (2016) detail the steps to drawing samples from the reward distribution based on the edit distance with stratified sampling. In this section we show how we sample from the Hamming distance (a special case of the edit distance) reward and how we handle large vocabularies to generate reasonable candidates. To draw from the Hamming distance reward, we proceed as follows:

1. Sample a distance d from $\{0, \dots, T\}$.
2. Pick d positions in the sequence to be changed among $\{1, \dots, T\}$.
3. Sample substitutions from a subset $\mathcal{V}_{sub}$ of the vocabulary ($|\mathcal{V}_{sub}| = V_{sub}$).

To sample a distance, we partition the set of sequences in $\mathcal{V}_{sub}$ terms $\mathcal{V}_{sub}^T$ with respect to their distance to the ground truth y^*:

$$\begin{cases} S_d = \{y \in \mathcal{V}_{sub}^T | \, d(y, y^*) = d\}, \\ \mathcal{V}_{sub}^T = \underset{d}{\cup} S_d, \\ \forall d, d' : S_d \cap S_{d'} = \emptyset. \end{cases}$$

To each distance d in $\{0, ..., T\}$ we assign the portion of rewards covered by S_d in $\mathcal{V}_{sub}^T$. Since all elements of S_d are assigned the same reward $e^{-\frac{d}{\tau}}$; we need only to multiply it by the set's size $|S_d|$. Counting the elements of $|S_d|$ is straight-forward: we choose d elements to alter in y^* $\left(\binom{T}{d}\text{combinations}\right)$ and at each position we have $(V_{sub} - 1)$ possibilities. The sampling distribution is obtained as:

$$p(d) = r(S_d)/r(\mathcal{V}_{sub}^T) \tag{20}$$

$$= \frac{\sum\limits_{y \in S_d} r(y|y^*)}{\sum\limits_{y \in \mathcal{V}_{sub}^T} r(y|y^*)}. \tag{21}$$

Given that $\{S_d\}_d$ form a partition of $\mathcal{V}_{sub}^T$,

$$\sum_{y \in \mathcal{V}_{sub}^T} r(y|y^*) = \sum_d \sum_{y \in S_d} e^{-\frac{d}{\tau}} \tag{22}$$

$$= \sum_d \binom{T}{d} (V_{sub} - 1)^d e^{-\frac{d}{\tau}} \tag{23}$$

$$= \left((V_{sub} - 1)e^{-\frac{1}{\tau}} + 1\right)^T, \tag{24}$$

we find:

$$p(d) = \binom{T}{d} \frac{(V_{sub} - 1)^d e^{-\frac{d}{\tau}}}{((V_{sub} - 1)e^{-\frac{1}{\tau}} + 1)^T}. \tag{25}$$

B Captioning

B.1 Experimental setup

Out of vocabulary words are replaced by <UNK> token and the captions longer than 16 words are truncated. As image encoding, we average-pool the features in the last convolutional layer of ResNet-152 (He et al., 2016) pre-trained on ImageNet. The 2048-dimensional image signature is further mapped to $\mathbb{R}^{512}$ to fit the word-embedding dimension, so it can be used as the first token fed to the RNN decoder. We use a single-layer RNN with $d = 512$ LSTM units.

For optimization, we use Adam (Kingma and Ba, 2015) with a batch size of 10 images, *i.e.* 50 sentences. We follow Lu et al. (2017); Pedersoli et al. (2017) and train in two stages: the first, optimizing the language model alone with an initial learning rate of 5e-4 annealed by a factor of 0.6 every 3 epochs starting from the 5th one. We train for up to 20 epochs with early stopping if CIDEr score on the validation set does not improve. In the second stage, we optimize the language model conjointly with $conv_4$ and $conv_5$ (the last 39 building blocks of ResNet-152) of the CNN model. The initial learning rate is of 6e-5 and diminishes by a factor of 0.8 every 4 epochs. The same early-stopping strategy is applied. For the token-level reward, we use GloVe (Pennington et al., 2014) as our word embedding, which we train on the captions in the MS-COCO training set. In preliminary experiments using the publicly available 300-dimensional GloVe vectors trained on Wikipedia 2014 + Gigaword worsens the model's results.

B.2 Restricted vocabulary sampling - supplementary results

In Table 4 we provide additional results for sequence-level smoothing, when using the BLEU-4 as reward function. We include results when computing BLEU-4 w.r.t. all reference sequences (like also done for CIDEr), and when computing w.r.t. a single randomly selected reference sentence (as is the case for Hamming). With the BLEU-4 reward, using $\mathcal{V}_{refs}$ yields best results in all but a single case. This underlines the effectiveness of sampling replacement words that are relevant to the task in sequence-level smoothing.

Captioning without attention					**Captioning with attention**				
Reward	$\mathcal{V}_{sub}$	BLEU-1	BLEU-4	CIDEr	Reward	$\mathcal{V}_{sub}$	BLEU-1	BLEU-4	CIDEr
Dirac		70.63	30.14	93.59	Dirac		73.40	33.11	101.63
Hamming	$\mathcal{V}$	71.76	31.16	96.37	Hamming	$\mathcal{V}$	73.12	32.71	101.25
Hamming	$\mathcal{V}_{batch}$	71.46	31.15	**96.53**	Hamming	$\mathcal{V}_{batch}$	73.26	**32.73**	101.90
Hamming	$\mathcal{V}_{refs}$	**71.80**	**31.63**	96.22	Hamming	$\mathcal{V}_{refs}$	**73.53**	32.59	**102.33**
BLEU-4 single	$\mathcal{V}$	71.30	31.11	96.11	BLEU-4 single	$\mathcal{V}$	72.98	32.55	101.15
BLEU-4 single	$\mathcal{V}_{batch}$	71.13	30.84	94.74	BLEU-4 single	$\mathcal{V}_{batch}$	72.98	32.48	101.05
BLEU-4 single	$\mathcal{V}_{refs}$	**71.78**	**31.63**	**97.29**	BLEU-4 single	$\mathcal{V}_{refs}$	**73.41**	**32.69**	**101.35**
BLEU-4	$\mathcal{V}$	71.56	**31.47**	96.56	BLEU-4	$\mathcal{V}$	73.39	32.89	102.60
BLEU-4	$\mathcal{V}_{batch}$	71.41	30.87	95.69	BLEU-4	$\mathcal{V}_{batch}$	73.24	32.74	102.49
BLEU-4	$\mathcal{V}_{refs}$	**72.08**	31.41	**97.21**	BLEU-4	$\mathcal{V}_{refs}$	**73.55**	**33.03**	**102.72**
CIDEr	$\mathcal{V}$	71.05	30.46	94.40	CIDEr	$\mathcal{V}$	73.08	32.51	101.84
CIDEr	$\mathcal{V}_{batch}$	71.51	31.17	95.78	CIDEr	$\mathcal{V}_{batch}$	**73.50**	**33.04**	**102.98**
CIDEr	$\mathcal{V}_{refs}$	**71.93**	**31.41**	**96.81**	CIDEr	$\mathcal{V}_{refs}$	73.42	32.91	102.23

Table 4: Captioning performance on MSCOCO when training with sequence-level loss smoothing.

B.3 Training time

We report below (Table 5) the average wall time to process a single batch (10 images *i.e.* 50 captions) when training the RNN language model with fixed CNN (without attention) on a Titan X GPU. We can clearly see that the lazy training is faster compared to the standard sequence smoothing and that the token-level smoothing does not hinder the training speed.

Loss	MLE	Tok	Seq	Seq lazy	Seq	Seq lazy	Seq	Seq lazy	Tok-Seq	Tok-Seq	Tok-Seq
Reward		Glove sim	Hamming								
$\mathcal{V}_{sub}$			$\mathcal{V}$	$\mathcal{V}$	$\mathcal{V}_{batch}$	$\mathcal{V}_{batch}$	$\mathcal{V}_{refs}$	$\mathcal{V}_{refs}$	$\mathcal{V}$	$\mathcal{V}_{batch}$	$\mathcal{V}_{refs}$
ms/batch	347	359	390	349	395	337	401	336	445	446	453

Table 5: Average training time per batch for different losses

B.4 Additional examples

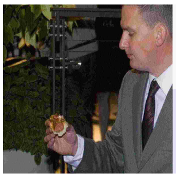

Ground truth:
a man holding a sausage dog and looking at the sausage do
a man in a suit stares at a chili dog with cheese
a man is eating a hot dog while wearing a suit
a man looks at a hot dog he is eating
a man holds up a partially eaten hotdog
Generated:
Baseline: a man holding a donut in his hand
Seq: a man eating a donut in a restaurant
Tok: a man holding a sandwich in his hands
Tok-Seq: a man holding a hot dog in his hand

Ground truth:
dirt bikes with lights on riding along a street with people watching from the side walk
the motorcycle procession made their way down the crowded street
police officers are on parade as crowds watch from aside
a group of motorcycles are going down the road
a line of police motorcycles driving down the road
Generated:
Baseline: a man riding a motorcycle down a street
Seq: a group of people riding bikes down a street
Tok: a group of people riding motorcycles down a street
Tok-Seq: a group of people riding motorcycles down a street

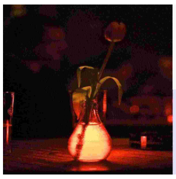

Ground truth:
a vase with a flower sitting on top of a wooden table
a flower vase with a glow to it sitting on a table
a small, illuminated vase holds a single tulip at a cafe
a weird and strange looking vase in a flower.
a single tulip is seen in a small vase
Generated:
Baseline: a glass vase with a candle in it
Seq: a glass vase sitting on top of a table
Tok: a vase with a flower in it on a table
Tok-Seq: a glass vase with a flower in it

Ground truth:
a background of blurred shapes is fronted by bunches of green bananas of which one's been
a bunch of small bananas still on the main branch
a large bunch of unripened green plantains on display
a picture of a bunches of green bananas
a bunch of bananas are piled together
Generated:
Baseline: a bunch of green bananas hanging from a tree
Seq: a bunch of green bananas on a tree
Tok: a bunch of green bananas hanging from a tree
Tok-Seq: a bunch of green bananas sitting on a table

Ground truth:
a man standing in front of a street vendor, a woman behind the counter
a man preparing food on a street cart next to a building
a man running a street stand in front of a yellow garag
a man and a woman stand at a portable vending cart
a woman eats a burger next to a street vendor
Generated:
Baseline: a man is standing next to a bicycle
Seq: a man on a bike with a man on the back
Tok: a couple of men standing next to each other
Tok-Seq: a man standing next to a woman in front of a store

Ground truth:
a colorful walk sign in the city is on a post
an intersection cross walk at greene street featuring the 'walk' ligh
view of street signs and an illuminated cross walk sign
the crosswalk sign is placed under a street sign
traffic signal for saying walk on greene st
Generated:
Baseline: a traffic light with a street sign on it
Seq: a street sign with a street sign on it
Tok: a traffic light and street sign on a pole
Tok-Seq: a traffic light and street sign on a pole

Ground truth:
there are two men standing on the beach with surf board
the two surfers are read to take on the waves
two surfers are standing on a beach holding their surfboards
a pair of surfers pause on a populated beach
two surfers with surfboards walk upon a beach
Generated:
Baseline: a couple of people standing on top of a beach
Seq: a couple of people that are on a beach
Tok: a couple of people standing on top of a beach
Tok-Seq: a couple of people that are holding surfboards

Ground truth:
a display case filled with bakes goods in front of a store
the front of a chinese store with some items on display
a chinese restaurant with a bunch of different plants near it.
a photo of an asian market with a display case
the counter of an ethnic asian cuisine bar
Generated:
Baseline: a display case filled with different types of donuts
Seq: a store filled with lots of fruit and vegetables
Tok: a display case filled with lots of donuts
Tok-Seq: a display case filled with lots of flowers

Ground truth:
the blossom of a plant hangs near large green leaves
small bananas growing on top of the banana tre
a weird looking tree filled with little miniature bananas
a large green leafy plant with a flower
a tree with tiny bananas growing on it
Generated:
Baseline: a close up of a bunch of green bananas
Seq: a tree with a bunch of bananas growing in it
Tok: a close up of a banana plant with leaves
Tok-Seq: a tree filled with lots of green bananas

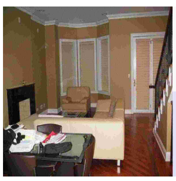

Ground truth:
a living room with a sectional couch, easy chair and glass desk covered in paper
home living room with brown walls with white trim, fireplace, and tan furnishings
a living room includes a beige sofa and a black fireplace
a couch and a chair in a small living room
a living area with sofa, chair and a fireplace
Generated:
Baseline: a living room filled with furniture and a large window
Seq: a living room filled with furniture and a tv
Tok: a living room with a couch and a desk
Tok-Seq: a living room filled with furniture and a fireplace

Ground truth:
a boy in a wet suit and a white and colored surfboar
a young child attempting to get onto a surfboard in the water
a young boy hanging on to a surfboard in the water
a young boy climbing into a surfboard in the water
a young man riding a surfboard in the ocean
Generated:
Baseline: a woman in the water with a surfboard
Seq: a woman is sitting on a surfboard in the water
Tok: a woman sitting on a surfboard in the water
Tok-Seq: a little boy that is standing in the water

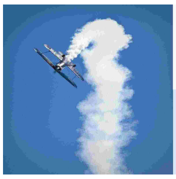

Ground truth:
the airplane in the sky is doing tricks while spitting out smoke.
a plane flies through the air with fumes coming out the back
an airplane is letting off white smoke against a blue sky
a biplane leaves a smoke trail while doing a trick
a biplane flying upside down leaving a large vapor trail
Generated:
Baseline: a plane flying through a blue sky with clouds
Seq: an airplane flying in the sky with smoke coming from it
Tok: a small plane flying through a blue sky
Tok-Seq: a small plane flying through a blue sky

Ground truth:
a close up of a giraffe eating from the top of a tree
a giraffe bending over in tall grass by some trees
a tall giraffe eating leafy greens in a jungle
a standing giraffe in tall brush eating leaves
giraffe leaning very far over to sample leaves
Generated:
Baseline: a giraffe standing next to a tree in a field
Seq: a couple of giraffe standing next to each other
Tok: a giraffe standing in the middle of a forest
Tok-Seq: a giraffe eating leaves from a tree

Ground truth:
a purple flower hanging upside down from a green stem with green plantains attache
a plant with a purple flower and several unripe bananas
a flower hanging from a bunch or green bananas
a banana plant and a bunch of green bananas
a flower with some plants on its stem
Generated:
Baseline: a bunch of bananas hanging from a tree
Seq: a close up of a flower on a tree
Tok: a bunch of green bananas hanging from a tree
Tok-Seq: a green flower is hanging from a banana tree

Ground truth:
a man with a jacket posing to throw a frisbee outside.
a man is throwing a frisbee in a sandy area
a man about to throw a frisbee by the road
a man wearing a baseball hat tossing a frisbee
a man in a baseball cap throwing a frisbee.
Generated:
Baseline: a man is holding a frisbee in a field
Seq: a man in a hat is holding a tennis racket
Tok: a man in a hat is holding a frisbee
Tok-Seq: a man with a frisbee in his hand

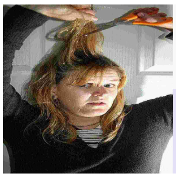

Ground truth:
a woman looks apprehensive as she prepares to cut her own hair with scissors.
a woman that is holding her hair and a pair of scissors
a lady cutting her own hair with a pair of huge scissor
there is a woman holding scissors to her hair
a young woman is curling her long hair
Generated:
Baseline: a woman in a black shirt and a black tie
Seq: a woman in a black shirt and black hair
Tok: a woman in a black shirt and a black tie
Tok-Seq: a woman holding a pair of scissors in her hand

Ground truth:
black and white image of white umbrellas hanging below light
several umbrellas are hanging upside down from a lighting system
a bunch of ornate lanterns are hanging on the cielin
a warehouse filled with light fixtures in it
there are many lights hanging from this ceilin
Generated:
Baseline: a bunch of umbrellas hanging from a ceiling
Seq: a bunch of umbrellas that are in a room
Tok: a bunch of umbrellas that are in a building
Tok-Seq: a bunch of umbrellas hanging from a ceiling

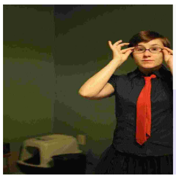

Ground truth:
the man wearing a red tie is standing near an animal's plastic house
a young girl wearing a red tie is adjusting her glasses.
the man in the red tie is putting on his glasses
a person with glasses and a tie in a room
a woman wearing glasses a shirt and ti
Generated:
Baseline: a man in a tie is holding a cell phone
Seq: a woman standing in a room talking on a phone
Tok: a woman wearing a red shirt and a tie
Tok-Seq: a woman in a red shirt and red tie

Ground truth:
a bathroom with a red wall and poster in front of a toilet
there is an indoor toilet underneath a sign that says please flush.
this bathroom has red and white walls and a poster
a toilet with a poster above it in a bathroo
a sign is seen posted above a toilet
Generated:
Baseline: a toilet with a sign attached to it
Seq: a bathroom with a toilet and a sign
Tok: a toilet in a bathroom with a sign above it
Tok-Seq: a bathroom with a toilet and a sign

Ground truth:
a cat lies on the couch next to a computer while holding a red stuffed toy
a black and white cat laying on a couch holding a stuffed animal
a sleepy cat on its back playing with a stuffed anima
a black and white cat is cuddled with a red toy
a black and white cat with a red stuffed toy
Generated:
Baseline: a black and white cat laying on a blanket
Seq: a black and white cat laying on a bed
Tok: a black and white cat laying on a bed
Tok-Seq: a black and white cat laying on top of a bed

Ground truth:
a young man in a sweat shirt is standing on a wooden walkway
a person riding a skate board on a wooden sidewal
a man is riding a skateboard across a bridge
a boy riding his skateboard down the wooden deck.
a man skateboarding across a small wooden bridge.
Generated:
Baseline: a man riding a skateboard on top of a wooden rail
Seq: a man riding a skateboard down a metal rail
Tok: a man standing on top of a wooden bench
Tok-Seq: a man riding a skateboard on top of a wooden rail

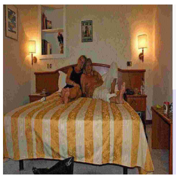

Ground truth:
a couple is smiling while posing for a picture on a bed
a couple laying on a big bed in a bedroom
an image of a couple in bed on gold sheet
two people laying in a neatly made be
a couple is lying on the bed
Generated:
Baseline: a woman sitting on a bed with a cat
Seq: a man sitting on a bed with a cat
Tok: a woman sitting on a bed in a bedroom
Tok-Seq: two people laying on a bed in a room

Ground truth:
two zebra's standing in a grassy field and one is eating grass
a zebra looking up as another grazes in a field
the zebras are grazing out in the field of grass.
a group of zebras stand together in a field
several zebras eating grass in a wildlife par
Generated:
Baseline: a couple of zebra standing on top of a grass covered field
Seq: a couple of zebra standing on top of a grass covered field
Tok: a couple of zebra standing next to each other on a field
Tok-Seq: a couple of zebras are standing in a field

Ground truth:
a man standing in front of a street vendor, a woman behind the counter
a man preparing food on a street cart next to a building
a man running a street stand in front of a yellow garag
a man and a woman stand at a portable vending cart
a woman eats a burger next to a street vendor
Generated:
Baseline: a man is standing next to a bicycle
Seq: a man on a bike with a man on the back
Tok: a couple of men standing next to each other
Tok-Seq: a man standing next to a woman in front of a store

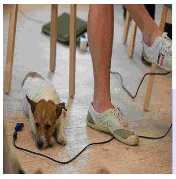

Ground truth:
a wooden floor with a dog laying down next to a persons feet and next to
a grown and white dog on floor next to person's shoes
a dog laying on the floor next to a persons legs
a little dog laying under the table at someones fee
a small dog laying next to a person wearing sneaker
Generated:
Baseline: a dog sitting on the floor with a pair of shoes
Seq: a dog and a pair of shoes on a floor
Tok: a dog laying on the ground next to a person
Tok-Seq: a dog is laying on the floor next to a persons feet

Ground truth:
a large, twin engine airliner is slightly tilted to one side in the air
it's wondrous how that big airplane manages to stay up in the sky
an air canada plane making a left turn in the sky
a plane flying through the air during a sunny da
a plane on the air flying very hig
Generated:
Baseline: a large jetliner flying through a blue sky
Seq: a large jetliner flying through a blue sky
Tok: a large jetliner flying through a blue sky
Tok-Seq: an airplane flying in the air with a sky background

Ground truth:
a broken door frame showing a a bathroom with a cement floor and a broken back
an outside doorway to a restroom showing a destroyed wall and damaged floor
a bathroom with walls that are falling down and a toilet
a doorway leading into a delapitated wall in a room
a doorway looking into a demolished bathroo
Generated:
Baseline: a dirty bathroom with a brick wall and a broken window
Seq: a door is open in a small room
Tok: a window that has a window in it
Tok-Seq: a dirty bathroom with a toilet and a window

Ground truth:
view from behind a tree of a lake and fall colored tress on the other side
a small boat near a wide river with a dense forest on the other sid
a snowy day in a colorful forest where leaves have already changed colors.
view from window across water with fall foliaged trees on other bank
a boat some water and some red and green tree
Generated:
Baseline: a view of a lake with a boat on it
Seq: a large body of water with a boat on it
Tok: a large body of water next to a forest
Tok-Seq: a view of a body of water with trees in the background

Ground truth:
a small glass of milk sitting next to a platter full of doughnuts
a cloth covered plate of donuts next to a glass of milk
the doughnuts are next to the glass of milk on the table
a couple of doughnuts sit next to a glass of milk
a savory snack of dounts with a glass of mil
Generated:
Baseline: a donut sitting on top of a wooden table
Seq: a close up of a doughnut on a plate
Tok: a donut and a drink on a table
Tok-Seq: a couple of donuts sitting on top of a table

Ground truth:
bread crumbs sitting on top of a veggie plate with noodles.
a plate of food that includes broccoli, noodles and bread crumbs
a plate of pasta with greens and toasted bread pieces.
a pasta dish with bread crumbs and cooked green vegetabl
a white plate topped with salad and onions
Generated:
Baseline: a close up of a plate of food with broccoli
Seq: a plate of food with broccoli and meat
Tok: a plate of food with meat and vegetables
Tok-Seq: a close up of a plate of food

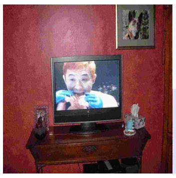

Ground truth:
a flat scree tv sitting on a wooden stand with an image of a ginger asian
a red headed man on a television in front of a red wall
a tv on a small table with pictures and figurines near b
an image of a living room setting with the tv o
a red painted wall is against a television
Generated:
Baseline: a television sitting on top of a wooden table
Seq: a flat screen tv mounted to a wall
Tok: a flat screen tv on a wooden table
Tok-Seq: a tv sitting on top of a wooden table

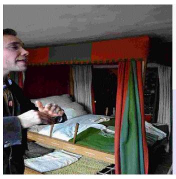

Ground truth:
a four poster bed covered with red and green curtains behind a ma
a man in his bedroom getting ready and a bed well mad
a man standing next to a bed while holding his hands together
a man standing near a bed with a red and green canopy
a man is standing near a canopy bed
Generated:
Baseline: a man sitting on a bed with a laptop
Seq: a man standing next to a bed covered in a blanket
Tok: a man sitting on a bed in a room
Tok-Seq: a man standing next to a bed with a canopy

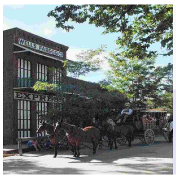

Ground truth:
a man is on a horse and carriage by wells fargo
a chariot pulled by horses carrying people outside a building
a man and woman in a four horse drawn carriag
there are horses pulling a man and a cart
a horse carriage and horses moving along a street
Generated:
Baseline: a group of horses pulling a carriage down a street
Seq: a group of horses pulling a carriage down a street
Tok: a group of horses are pulling a carriage
Tok-Seq: a couple of horses pulling a carriage down a street

Ground truth:
a red and white plane flying under a blue sk
an orange, red and grey plane flying in the sky
a large jetliner flying through a cloudy blue sky
a airplane that is flying in the sky
the jet airplane flies across the blue sky.
Generated:
Baseline: an airplane flying in the sky with a sky background
Seq: a red and white plane flying in the sky
Tok: a plane flying in the air with a sky background
Tok-Seq: a red and white airplane flying in the sky

Ground truth:
a platter of raw vegetable crudites and dip sits on a table with other condiments.
a snack plate with dip carrots celery tomatoes pickles and cucumber on a tabl
a platter topped with sliced vegetables with ranch dip in the center
vegetable tray that contains carrots, cucumbers, peppers, tomatoes and celer
a vegetable platter with dip on a table
Generated:
Baseline: a plate of food including carrots and carrots
Seq: a table topped with a variety of vegetables
Tok: a plate of food with carrots and carrots
Tok-Seq: a table topped with lots of different vegetables

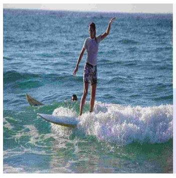

Ground truth:
a surfer standing on their board in relatively calm water
a woman riding a wave on top of a surfboard
a woman is on her surfboard in the water
she is well balanced on her new surfboard
a man that is surfing in some wate
Generated:
Baseline: a man on a surfboard in the water
Seq: a man on a surfboard in the water
Tok: a man riding a wave on top of a surfboard
Tok-Seq: a woman riding a wave on top of a surfboard

Ground truth:
a teenaged boy poses on the beach with his surfboard
a man stands on a beach with a surf board
a man poses with a surfboard on a beach
a man is standing next to a surfboard outsid
a guy on a beach holding a surf board
Generated:
Baseline: a man holding a surfboard on a beach
Seq: a man standing on a beach holding a surfboard
Tok: a man standing on a beach holding a surfboard
Tok-Seq: a man standing on a beach holding a surfboard

Ground truth:
a pizza that appears to be burned and has olives on it
a square shaped pizza with olives on it is over baked.
there is a pizza with cheese and olives on it
a rectangular pizza with cheese and olives sprinkled over it
a rectangular pizza with an egg on top
Generated:
Baseline: a close up of a pizza on a plate
Seq: a close up of a pizza on a plate
Tok: a pizza sitting on top of a white plate
Tok-Seq: a close up of a pizza on a table

Ground truth:
a couple of kids playing with a racquet in front of a the camera
a couple of girls sitting on a bench with tennis racquets
two kids holding tennis rackets while standing in a garage
two little girls and white uniforms holding up tennis rackets.
two young blonde girls sitting and holding tennis rackets
Generated:
Baseline: a woman and a little girl holding tennis rackets
Seq: a couple of kids standing next to each other
Tok: a woman and a child holding tennis rackets
Tok-Seq: two little girls sitting next to each other holding tennis rackets

Ground truth:
a man with safety equipment next to a fallen tree and red fire hydrant
the man is cutting down the trees around the red fire hydrant.
a worker standing next to a tree that's been chopped down.
a man standing by a tree and a fire hydrant
the man is cutting trees down outside.
Generated:
Baseline: a man standing next to a fire hydrant
Seq: a man sitting on a rock in the woods
Tok: a man sitting on a log in the woods
Tok-Seq: a man standing next to a red fire hydrant

C Neural machine translation

C.1 Experimental setups

WMT14 English-to-French We use the same experimental setting as Bahdanau et al. (2015): 12M paired sentences are used for training, 6,003 pairs for validation (news-test-2012 and news-test-2013) and 3,003 test pairs (news-test-2014). After tokenization, 30k most frequent tokens are selected for the model's vocabulary. We use an attentive encoder-decoder with a 2-layers bi-directionnal encoder of dimension $d = 2000$ and a single-layer decoder of dimension $d = 2000$ as well. We use batches of size 80 and train for 3 epochs with Adam (Kingma and Ba, 2015) starting with a learning rate of 2e-4. To generate translations we use beam search of size five.

IWSLT14 German-to-English We use the same settings as (Ranzato et al., 2016); the training set consists of 153k sentence pairs and 7k pairs are assigned to the validation and test sets. After tokenization and lower-casing, we remove sentences longer than 50 tokens. The English vocabulary has 22,822 words while the German has 32,009 words. We use an attentive encoder-decoder with a single bi-directionnal encoder and decoder of dimension $d = 128$. To generate translations we use beam search of size five. We use batches of size 32 and train for 40 epochs with Adam (Kingma and Ba, 2015) starting with a learning rate of 1e-3.

C.2 Examples

Source (en)	I think it's conceivable that these data are used for mutual benefit .
Target (fr)	J'estime qu'il est concevable que ces données soient utilisées dans leur intérêt mutuel .
MLE	Je pense qu'il est possible que ces données soient utilisées à des fins réciproques .
Tok-Seq	Je pense qu'il est possible que ces données soient utilisées pour le bénéfice mutuel .
Source (en)	However , given the ease with which their behaviour can be recorded , it will probably not be long before we understand why their tails sometimes go one way , sometimes the other .
Target (fr)	Toutefois , étant donné la facilité avec laquelle leurs comportements peuvent être enregistrés , il ne faudra sûrement pas longtemps avant que nous comprenions pourquoi leur queue bouge parfois d'un côté et parfois de l'autre .
MLE	Cependant , compte tenu de la facilité avec laquelle on peut enregistrer leur comportement , il ne sera probablement pas temps de comprendre pourquoi leurs contemporains vont parfois une façon , parfois l'autre .
Tok-Seq	Cependant , compte tenu de la facilité avec laquelle leur comportement peut être enregistré , il ne sera probablement pas long avant que nous ne comprenons la raison pour laquelle il arrive parfois que leurs agresseurs suivent un chemin , parfois l'autre .
Source (en)	The public will be able to enjoy the technical prowess of young skaters , some of whom , like Hyeres' young star , Lorenzo Palumbo , have already taken part in top-notch competitions .
Target (fr)	Le public pourra admirer les prouesses techniques de jeunes qui , pour certains , fréquentent déjà les compétitions au plus haut niveau , à l'instar du jeune prodige hyérois Lorenzo Palumbo .
MLE	Le public sera en mesure de profiter des connaissances techniques des jeunes garçons , dont certains , à l'instar de la jeune star américaine , Lorenzo , ont déjà participé à des compétitions de compétition .
Tok-Seq	Le public sera en mesure de profiter de la finesse technique des jeunes musiciens , dont certains , comme la jeune star de l'entreprise , Lorenzo , ont déjà pris part à des compétitions de gymnastique .

Table 7: WMT'14 English-to-French examples

Source (de)	sie repräsentieren teile der menschlichen vorstellungskraft , die in vergangene zeiten <UNK> . und für alle von uns , werden die träume dieser kinder , wie die träume unserer eigenen kinder teil der geographie der hoffnung .
Target (en)	they represent branches of the human imagination that go back to the dawn of time . and for all of us , the dreams of these children , like the dreams of our own children , become part of the naked geography of hope .
MLE	they represent parts of the human imagination that were blogging in the past time , and for all of us , the dreams of these children will be like the dreams of our own children part of hope .
Tok-Seq	and they represent parts of the human imagination that live in past times , and for all of us , the dreams of these children , like the dreams of our own children are part of hope .
Source (de)	und ja , vieles von dem , was heute gesagt wurde , berührt mich sehr , weil viele , viele schöne äußerungen dabei waren , die ich auch durchlebt habe .
Target (en)	and yes , a lot of what is said today really moves me , because many , many nice statements were made , which i also was part of .
MLE	and yes , a lot of what 's been said to me today , i got very , very , very , very beautiful expressions that i used to live through .
Tok-Seq	and yes , a lot of what 's been told today is very , very much , because many , lots of beautiful statements that i 've been through .
Source (de)	noch besser , er wurde in <UNK> nach den angeblich höchsten standards der nachhaltigkeit gezüchtet .
Target (en)	even better , it was <UNK> to the supposed highest standards of sustainability .
MLE	even better , he has been bred in love with the highest highest standards of sustainability .
Tok-Seq	even better , he was raised in terms of dignity , the highest standards of sustainability .

Table 8: IWSLT'14 German-to-English examples